

Non-Perturbative Dynamical Effects in Nearly Scale Invariant Systems: The Action of Breaking Scale Invariance

Jeff Maki¹, Li-Ming Zhao^{1,2}, and Fei Zhou¹

1) *Department of Physics and Astronomy, University of British Columbia, Vancouver V6T 1Z1, Canada*

2) *Center for Theoretical Physics, Capital Normal University, Beijing, China*

(Dated: December 14, 2024)

In this work we develop a general formalism that categorizes the action of breaking the scale invariance in the non-equilibrium dynamics of non-relativistic quantum systems. This approach is equally applicable to both strongly and weakly interacting systems. We show that any small deviation from the strongly interacting fixed point leads to non-perturbative effects in the long time dynamics, dramatically altering the dynamics at the scale invariant fixed point. As a concrete example, we apply this approach to the non-equilibrium dynamics of a non-interacting quantum gas in the presence of an impurity, and for the interacting two-body problem, both in three spatial dimensions. Near the resonantly-interacting scale invariant fixed point, we show that the dynamics are altered by a non-perturbative log-periodic beat. The presence of the beat is universal and depends only on deviating from the resonant fixed point, while the frequency depends on the microscopic parameters of the system.

I. INTRODUCTION

Ever since the creation of atomic gases, the study of their non-equilibrium dynamics has been a rewarding pursuit. In recent years, the technological prowess displayed in experiments has allowed for an unprecedented study in dynamics. The number of dynamical studies available cover a plethora of phenomena, ranging from quench dynamics [1–4], thermalization and localization [3, 5–7], and periodic driving [8–10]. On the theoretical side, there has been considerable progress in understanding these dynamical phenomena [3, 10–14], but often this is limited to numerical or semi-classical methods.

One fruitful approach for understanding such a complex problem is symmetry. The presence of symmetries in a system will undoubtedly lead to simplifications. One such symmetry that still peaks the interest of theorists and experimentalists alike is the symmetry associated with scale invariance. When a system possesses scale invariance, the governing equations of motion remain unchanged when subject to dilations of the spatial and temporal coordinates:

$$\vec{r}'_i = b\vec{r}_i \quad i = 1, 2, \dots, N \quad t' = b^2 t, \quad (1.1)$$

where $\{\vec{r}_i\}$ denotes the position of the N particles in the system with $i = 1, 2, \dots, N$, and b is a scaling factor.

Thankfully, cold atoms offer a number of controllable scale invariant and nearly scale invariant systems; such as the two dimensional quantum gas [15–18], the three dimensional degenerate Fermi gas at unitarity [19–21], the three dimensional degenerate Bose gas at unitarity [4], and the two-dimensional Fermi gas at a p-wave resonance [22]. For these systems, scale invariance has been applied to obtain universal relations for quantities such as the equation of state, and bulk viscosity [22–24]. The application of scale invariance in cold atoms is a strong motivation for a more systematic study of scale symmetry in non-equilibrium dynamics.

The primary method for theoretically understanding the dynamics of interacting cold atom systems has been the scaling solution [25–28]. The scaling solution is a variational approach that is often applied to semiclassical approximations. Although the interacting quantum gas is generally not scale invariant, it was noticed that the scaling solution provides an approximate description of the dynamics [29]. An extension of this approach to examine the effects of broken scale invariance on the dynamics of a two dimensional Bose gas with attractive interactions was presented in Ref. [30].

One of the first attempts at understanding the role of scale invariance on fully quantum dynamics was presented in Ref. [31]. In this work, the motion of the moment of inertia was examined for an interacting two-dimensional Bose gas in a harmonic trap. This system was shown to have an approximate hidden SO(2,1) symmetry. This approximate symmetry is related to conformal symmetry up to the quantum anomaly [32–34]. In terms of the moment of inertia, it was shown that the exact symmetry fixes the frequency of the breathing mode at twice the trap frequency. Even though it was first predicted for bosons, this approximate symmetry is present for two-dimensional Fermi gases, [31, 35], and has been observed experimentally for both bosons and fermions [17, 36]. More recently, the role of scale invariance on the dynamics of quantum gases in time dependent harmonic traps was studied experimentally, [37].

A full description of scale invariant quantum dynamics can be provided by the general equations of motion. Equations of motion are useful for addressing the role of scale invariance on the dynamics of a global observable [31–34, 37, 38]. However this approach becomes rather difficult, if not unsolvable, when the system is not fine tuned to scale invariance. In addition, this approach does not include much local space-time information that is contained in the wave function itself. A microscopic approach, which takes into account the SO(2,1) symmetry on the many body wave function, was put forward in

Ref. [39]. In particular, this approach has been used to study both the energetics and dynamics of unitary Fermi gases in three dimensions [39, 40], of the Tonks gas in one dimension [41], and for harmonically trapped scale invariant systems [42].

For a given physical system, scale invariance occurs at the fixed points of the renormalization group flow [43, 44]. Most systems will possess multiple fixed points, each characterized by their own infra-red stabilities and critical exponents. In the context of three dimensional cold gases, there are two fixed points available: the non-interacting and resonantly-interacting quantum gas. When a system resides at a fixed point, certain dynamics, following the Heisenberg equations of motion, will be dictated by the scale symmetry alone, and neither on the stability of the fixed point, nor the microscopic features of the system.

This begs the question, how the non-equilibrium dynamics near a given fixed point will be affected by the stability and universality class of that fixed point. Will the non-equilibrium dynamics be completely equivalent near different fixed points, or will they fall into their own stability and universality class? To perform such a study one must extend the analysis of dynamics, not only to the resonant fixed point, but also to the vicinity of the fixed point, where the scale symmetry is broken explicitly, but slightly. Although there has been numerous theoretical studies on strongly interacting quantum gases using scale symmetry [23, 24, 45–47], a complete understanding of three-dimensional resonant quantum gases has yet to be achieved. It is not surprising that the categorization of the dynamics near the different scale invariant fixed points has been uncharted waters for theorists.

This is the first in a series of works to examine the consequences of conformal symmetry and its breaking on non-equilibrium quantum dynamics. In this article we lay down the general framework for categorizing the dynamics near a given fixed point. This formalism is valid for arbitrary number of particles, regardless of their statistics. We show that the dynamics do indeed depend upon whether one deviates from the resonantly-interacting or non-interacting fixed point. To perform this study, we employ the microscopic wave function which explicitly exhibits conformal symmetries. This approach is useful for studying nearly scale invariant dynamics, as it expands the dynamics in terms of a complete set of wave functions whose unitary evolution is equivalent to a time dependent rescaling.

As a concrete example we employ this formalism to study the dynamics of two systems: the non-interacting quantum gas in the presence of a short ranged impurity, and the two-body problem with short ranged interactions, both in three spatial dimensions. In general, these two systems are not scale invariant, thanks to the presence of an additional length scale, the scattering length, a . However, when a is infinite or zero, these systems will become scale invariant. In cold atom experiments both scale invariant fixed points can be achieved thanks to

the presence of Feshbach resonances [2]. The application of this approach to many body systems and the classification of relevant-irrelevant actions near a conformal symmetric fixed point will be presented in a forthcoming article.

For the two examples discussed above, we find that the dynamics near the resonant fixed point are fundamentally different in comparison to the dynamics at the resonant fixed point itself. Near resonance, the scale invariant dynamics are broken by a log-periodic beat, the presence of which is non-perturbative, universal, and depends only on deviating from the resonant fixed point. Although, the frequency of the beat depends on the finite range of the potential. This behaviour is not present for weak interactions where the long time dynamics are qualitatively similar to the scale invariant dynamics.

The remainder of the article is organized as follows: in Section II we review the many body wave function. The dynamics of scale invariant systems are studied in Section III. The general formalism for describing the non-equilibrium dynamics near a fixed point is then given in Sec. IV. In Sec. V we consider the dynamics for the non-interacting quantum gas in the presence of an impurity. The dynamics of the two body problem are then considered in Sec. VI. We then conclude with a discussion of the results in Section VII.

II. DYNAMICS IN AN EXPANDING NON-INERTIAL REFERENCE FRAME

We begin by examining the time dependent many body Schrodinger equation for a system of N particles with spin-independent interactions, $V(\vec{r})$, and in an external potential, $U(\vec{r})$, in three spatial dimensions:

$$i\partial_t\psi(\{\vec{r}_i, \sigma_i\}, t) = H\psi(\{\vec{r}_i, \sigma_i\}, t),$$

$$H = \sum_i \left[-\frac{1}{2}\nabla_i^2 + U(\vec{r}_i) \right] + \frac{1}{2} \sum_{i,j} V(\vec{r}_i - \vec{r}_j), \quad (2.1)$$

where the atomic mass, m , and \hbar have been set to unity. \vec{r}_i and σ_i designate the position and spin of the i th particle, respectively.

For systems with scale invariance or that are nearly scale invariant, it is convenient to introduce the wave function:

$$\psi(\{\vec{r}_i, \sigma_i\}, t) = \frac{1}{\lambda^{3N/2}(t)} e^{\frac{i}{2} \sum_i \tau_i^2 \dot{\lambda}(t)/\lambda(t)} \phi\left(\left\{\frac{\vec{r}_i}{\lambda(t)}, \sigma_i\right\}, \tau(t)\right). \quad (2.2)$$

In Eq. (2.2), $\lambda(t)$ is a time dependent scaling factor with units of length, and $\tau(t)$ is a dimensionless effective time. The wave function, $\phi(\{\vec{r}_i/\lambda(t), \sigma_i\}, \tau(t))$, contains all the many body information of the original wave function,

and is both appropriately symmetrized and normalized. This wave function was first introduced in Ref. [39]. The validity of this wave function for non-relativistic quantum systems was discussed in Ref. [48].

Eq. (2.2) is motivated by the scale transformation given by Eq. (1.1). It combines a time dependent rescaling of the spatial coordinates with a gauge transforma-

tion. The effect of this combination is to separate the simple rescaling dynamics governed by $\lambda(t)$ from the non-trivial dynamics governed by $\tau(t)$.

After substituting Eq. (2.2) into the time dependent Schrodinger equation, Eq. (2.1), one finds a Schrodinger-like equation for the field $\phi(\{\vec{r}_i/\lambda(t), \sigma_i\}, \tau)$:

$$i \frac{\partial \tau}{\partial t} \frac{\partial}{\partial \tau} \phi(\{\vec{x}_i, \sigma_i\}, \tau(t)) = \left(\sum_i \left[-\frac{1}{2} \frac{1}{\lambda^2(t)} \tilde{\nabla}_i^2 + \frac{x_i^2}{2} \ddot{\lambda}(t) \lambda(t) + U(\lambda(t) \vec{x}_i) \right] + \frac{1}{2} \sum_{i,j} V(\lambda(t) (\vec{x}_i - \vec{x}_j)) \right) \phi(\{\vec{x}_i, \sigma_i\}, \tau(t)). \quad (2.3)$$

The effective spatial and temporal coordinates in Eq. (2.3) are defined as:

$$\vec{x}_i = \vec{r}_i/\lambda(t), \quad i = 1, 2, \dots, N \quad \tau(t), \quad (2.4)$$

respectively, and the operator, $\tilde{\nabla}_i$, acts on the effective position, \vec{x}_i . In order for the dynamics after the transformation, Eq. (2.3), to be identical to a Schrodinger equation, the time derivative and the kinetic energy must scale in the same way. For this reason, it is necessary to choose:

$$\frac{\partial \tau(t)}{\partial t} = \frac{1}{\lambda^2(t)}. \quad (2.5)$$

One can then derive a Schrodinger equation for the field $\phi(\{\vec{x}_i, \sigma_i\}, \tau)$ in terms of the effective coordinates:

$$i \frac{\partial}{\partial \tau} \phi(\{\vec{x}_i, \sigma_i\}, \tau) = \tilde{H}(\tau) \phi(\{\vec{x}_i, \sigma_i\}, \tau),$$

$$\tilde{H}(\tau) = \sum_i \left[-\frac{1}{2} \tilde{\nabla}_i^2 + \frac{x_i^2}{2} \ddot{\lambda}(t(\tau)) \lambda^3(t(\tau)) + \lambda^2(\tau) U(\lambda(\tau) \vec{x}_i) \right]$$

$$+ \frac{1}{2} \sum_{i,j} \lambda^2(\tau) V(\lambda(\tau) (\vec{x}_i - \vec{x}_j)). \quad (2.6)$$

At this stage, the choice of $\lambda(t)$ is arbitrary. The optimal choice of $\lambda(t)$ for the present discussion is to eliminate the time dependence in the harmonic term by setting:

$$\ddot{\lambda}(t) \lambda^3(t) = 1, \quad \lambda(0) = \lambda_0, \quad \dot{\lambda}(0) = 0, \quad (2.7)$$

where λ_0 is the length scale describing the initial wave function. The initial conditions are chosen such that the initial wave function in the laboratory frame is related to the initial effective wave function via: $\psi(\{\vec{r}_i\}, 0) = \lambda_0^{-3N/2} \phi(\{\vec{r}_i/\lambda_0\}, 0)$. The solution to Eqs. (2.5) and (2.7) is:

$$\lambda(t) = \lambda_0 \sqrt{1 + \frac{t^2}{\lambda_0^4}}, \quad \tau(t) = \arctan\left(\frac{t}{\lambda_0^2}\right),$$

$$\lambda(\tau) = \lambda_0 \sec(\tau), \quad 0 \leq \tau < \pi/2. \quad (2.8)$$

Substituting the solution for $\lambda(t)$ into Eq. (2.6) gives the effective Schrodinger equation:

$$i \frac{\partial}{\partial \tau} \phi(\{\vec{x}_i, \sigma_i\}, \tau) = \tilde{H}(\tau) \phi(\{\vec{x}_i, \sigma_i\}, \tau),$$

$$\tilde{H}(\tau) = \sum_i \left[-\frac{1}{2} \tilde{\nabla}_i^2 + \frac{x_i^2}{2} + \lambda^2(\tau) U(\lambda(\tau) \vec{x}_i) \right]$$

$$+ \frac{1}{2} \sum_{i,j} \lambda^2(\tau) V(\lambda(\tau) (\vec{x}_i - \vec{x}_j)). \quad (2.9)$$

This is just the Schrodinger equation for an interacting quantum gas in a harmonic trap. Physically, this transformation is equivalent to studying the dynamics in an expanding non-inertial reference frame with coordinates given by Eq. (2.4). The harmonic potential in Eq. (2.9) is simply a fictitious force which appears because one is working in this expanding non-inertial reference frame. The penalty for using this transformation is that the external potential and the interactions now acquire time dependence.

III. DYNAMICS AT A SCALE INVARIANT FIXED POINT

When a quantum system possesses scale invariance, the Schrodinger equation in the laboratory frame, Eq. (2.1), is invariant under Eq. (1.1). For this to be true, a scale invariant Hamiltonian in the laboratory frame, H_s , must rescale like the time derivative:

$$H'_s = b^{-2} H_s. \quad (3.1)$$

This implies that for a system to be scale invariant, any potential must scale like the kinetic energy. That is, a

scale invariant external potential, $U_s(\vec{r})$, and interaction potential, $V_s(\vec{r})$, must satisfy:

$$U_s(b\vec{r}) = b^{-2}U_s(\vec{r}), \quad V_s(b\vec{r}) = b^{-2}V_s(\vec{r}), \quad (3.2)$$

for some scaling factor, b . The main consequence of Eq. (3.2) on Eq. (2.9), is that any scale invariant Hamiltonian in the laboratory frame, H_s , will transform into a time independent Hamiltonian in the non-inertial reference frame, \tilde{H}_s :

$$\tilde{H}_s = \sum_i \left[-\frac{1}{2}\tilde{\nabla}_i^2 + \frac{x_i^2}{2} + U_s(\vec{x}_i) \right] + \frac{1}{2} \sum_{i,j} V_s(\vec{x}_i - \vec{x}_j). \quad (3.3)$$

Another consequence of scale invariance is the presence of the conformal tower. At any fixed point, Eq. (2.9) possesses the $SO(2,1)$ symmetry [39, 49–51]. One can show that the symmetry guarantees that the spectrum of Eq. (3.3) contains a series of evenly spaced states with energies:

$$E_n = 2n + E_0 \quad n = 0, 1, 2, \dots \quad (3.4)$$

This spectrum is known as the conformal tower. In general, there can be multiple conformal towers present, each with a different ground state energy, E_0 . In terms of dynamics, the breathing modes in two-dimensional quantum gases are an approximate conformal tower, a result of the approximate $SO(2,1)$ symmetry [17, 31, 35, 36].

It is now possible to study the dynamics of a scale invariant quantum system. To begin, we expand the initial wave function, $\psi_0(\{\vec{r}_i\})$ [52], in terms of the eigenstates of Eq. (3.3) for a given fixed point, and perform the standard unitary time evolution:

$$\phi(\{\vec{x}_i\}, \tau) = \sum_n C_n \phi_n(\{\vec{x}_i\}) e^{-iE_n \tau}, \quad (3.5)$$

where the state, $\phi_n(\{\vec{x}_i\})$, is an eigenstate of Eq. (3.3) at a given fixed point with energy, E_n , given by Eq. (3.4). The expansion coefficients for the initial wave function are given by C_n , which we assume to be real for the remainder of the article. The benefit of using this basis can be seen by preparing the system in a single eigenstate. In this case the dynamics in the non-inertial reference frame is a trivial gauge transformation. This implies that for a state initially prepared with a given $n = 0, 1, 2, 3, \dots$, the dynamics in the laboratory frame, see Eq. (2.2), possess a scaling solution:

$$|\psi(\{\vec{r}_i\}, t)|^2 = \frac{1}{\lambda^{3N}(t)} |\phi_n(\{\frac{\vec{r}_i}{\lambda(t)}\})|^2. \quad (3.6)$$

where $\lambda(t)$, which depends on the initial conditions, see Eq. (2.8), is the scaling parameter. Eq. (3.6) states that

the time evolved wave function maintains the same shape as the initial wave function, exactly like a Gaussian wave packet. Such shape preserving eigenstates have been applied to the study of the unitary Fermi gas in three spatial dimensions [39, 40], and the Tonks gas in one dimension [41].

More generally, the initial wave function will be a superposition of eigenstates. For this situation, one can still make a general statement about the dynamics. To do so, we note that in this non-inertial reference frame, the effective time coordinate, τ , defined in Eq. (2.8), is bounded: $0 \leq \tau < \pi/2$. In the long time limit, $t \gg \lambda_0^2$, the effective time coordinate, τ , quickly saturates at $\pi/2$. This states that the long time dynamics in the laboratory frame can be obtained by taking the limit as τ approaches $\pi/2$ in Eq. (3.5). At the scale invariant point, there can be no singular behaviour near $\pi/2$. One can then simply set $\tau = \pi/2$, in Eq. (3.5), and the wave function in the non-inertial reference frame freezes.

The fact that the wave function freezes for arbitrary superposition means that the unitary time evolution in the laboratory frame, Eq.(2.2), is equivalent to a time dependent rescaling in the long time limit:

$$\begin{aligned} |\psi(\{\vec{r}_i\}, t_2)|^2 &\approx \left(\frac{\lambda(t_1)}{\lambda(t_2)} \right)^{3N} \left| \psi \left(\{\vec{r}_i\} \frac{\lambda(t_1)}{\lambda(t_2)}, t_1 \right) \right|^2, \\ |\psi(\{\vec{r}_i\}, t_1)|^2 &\approx \frac{1}{\lambda^{3N}(t_1)} \left| \phi \left(\left\{ \frac{r_i}{\lambda(t_1)} \right\}, \pi/2 \right) \right|^2. \end{aligned} \quad (3.7)$$

where N is the number of particles, and both $t_1, t_2 \gg \lambda_0^2$. The only difference between Eq. (3.6) and Eq. (3.7) is that the shape of the wave function for an arbitrary superposition at long times is not necessarily equivalent to the initial wave function.

This approximate rescaling of the dynamics leads to important conclusions for the dynamics of local observables. In particular, the expectation value of a local observable $O(\{\vec{r}_i\})$, with scaling dimension d_O , will also possess a scaling solution in the long time limit:

$$\begin{aligned} \lim_{t \rightarrow \infty} \langle O \rangle(t) &= \int \frac{d^3 r_1}{\lambda^3(t)} \dots \frac{d^3 r_N}{\lambda^3(t)} \left| \phi \left(\left\{ \frac{\vec{r}_i}{\lambda(t)} \right\}, \tau(t) \right) \right|^2 O(\{\vec{r}_i\}), \\ &= \frac{1}{\lambda(t)^{d_O}} \int d^3 x_1 \dots d^3 x_N |\phi(\{\vec{x}_i\}, \pi/2)|^2 \tilde{O}(\{\vec{x}_i\}), \\ &= \frac{1}{\lambda^{d_O}(t)} \langle \tilde{O} \rangle(\pi/2), \end{aligned} \quad (3.8)$$

where $\langle \tilde{O} \rangle(\pi/2)$ is the asymptotic expectation value of the operator in the non-inertial reference frame.

To give a more concrete example, consider the moment of inertia operator, r^2 :

$$\begin{aligned}
r^2 &\equiv \frac{1}{N} \sum_{i=1}^N r_i^2 \\
\lim_{t \rightarrow \infty} \langle r^2 \rangle(t) &= \lambda^2(t) \int d^3 x_1 \dots d^3 x_N |\phi(\{\vec{x}\}_i, \pi/2)|^2 x_1^2, \\
&= \lambda^2(t) \langle x^2 \rangle(\pi/2), \tag{3.9}
\end{aligned}$$

where $\langle x^2 \rangle(\tau)$ is the moment of inertia in the non-inertial reference frame. As discussed previously, the dynamics in the non-inertial reference frame freeze, and the dynamics of Eq. (3.9) is controlled by the simple rescaling dynamics of $\lambda(t)$, equivalent to Eq. (3.8).

IV. DYNAMICS NEAR A SCALE INVARIANT FIXED POINT

In this section we put forward a general formalism for studying the dynamics near a scale invariant fixed point. This discussion does not depend on the number of particles or their statistics, only on the deviation from scale invariance. We first write the effective Hamiltonian in Eq. (2.9), $\tilde{H}(\tau)$, as a sum of two parts:

$$\tilde{H}(\tau) = \tilde{H}_s + \delta\tilde{H}(\tau), \tag{4.1}$$

where \tilde{H}_s is the scale invariant Hamiltonian transformed into the non-inertial reference frame, Eq. (3.3), and $\delta\tilde{H}(\tau)$ is the deviation from \tilde{H}_s . As seen by (3.3), \tilde{H}_s is time independent due to the scale symmetry in the laboratory frame. The matrix elements of Eq. (4.11), with respect to the eigenstates of \tilde{H}_s , will depend on the nearby fixed point.

For the most general deviation that we want to consider, the deviation operator in the non-inertial reference frame can be written in the form:

$$\delta\tilde{H}(\tau) = \delta\tilde{h} \left(\frac{\lambda(\tau)}{a} \right)^\alpha = \delta\tilde{h} \left(\frac{\lambda_0}{a} \right)^\alpha \sec^\alpha(\tau). \tag{4.2}$$

where α is the negative of the scaling dimension of the deviation, a is a length scale introduced to make the deviation, and $\delta\tilde{h}$ is a universal, time-independent, dimensionless, operator that only depends on the number of particles, N . In Appendix A, explicit calculations can be found for the deviation near the resonant, and non-interacting fixed points, for both the non-interacting quantum gas in the presence of an impurity, and for the two-body problem.

To solve the time dependent Schrodinger equation near a given fixed point, in the non-inertial reference frame, Eq. (2.9), it is convenient to use the interaction picture with respect to \tilde{H}_s . The fact that we are using \tilde{H}_s as a reference Hamiltonian does not alter the application of

the interaction picture. The solution to Eq. (2.9) using the interaction picture is given by [53]:

$$\begin{aligned}
\phi(\{\vec{x}_i\}, \tau) &= \sum_n C_n(\tau) e^{-iE_n\tau} \phi_n(\{\vec{x}_i\}), \\
C_n(\tau) &= \langle n | T e^{-i \int_0^\tau d\tau' \delta\tilde{H}_I(\tau')} | \psi_0 \rangle, \\
\delta\tilde{H}_I(\tau) &= e^{i\tilde{H}_s\tau} \delta\tilde{H}(\tau) e^{-i\tilde{H}_s\tau}, \tag{4.3}
\end{aligned}$$

where $\langle \{\vec{x}_i\} | n \rangle = \phi_n(\{\vec{x}_i\})$ are the eigenstates of Eq. (3.3) with energies given by Eq. (3.4), $\langle \{\vec{r}_i\} | \psi_0 \rangle = \lambda_0^{-3N/2} \phi(\{\vec{r}_i/\lambda_0\})$ is the initial wave function, and T represents the time ordering operator.

Although Eq. (4.3) gives the exact solution, it is instructive to first consider the results from time-dependent perturbation theory. For $\alpha \geq 1$, the interaction diverges as: $(\pi/2 - \tau)^{-\alpha}$, in the long time limit, i.e. when $t \gg \lambda_0^2$, or equivalently, when τ approaches $\pi/2$. This divergence will lead to a breakdown of perturbation theory at long times. To clearly see this, consider the expansion coefficients at long times, to first order in perturbation theory, for $\alpha = 1$:

$$\begin{aligned}
C_n(\tau) &\approx C_n(0) - i \frac{\lambda_0}{a} \log \left(\frac{1}{\pi/2 - \tau} \right) \\
&\cdot \langle n | e^{-i\tilde{H}_s\pi/2} \delta\tilde{h} e^{-i\tilde{H}_s\pi/2} | \psi_0 \rangle + \dots \tag{4.4}
\end{aligned}$$

As seen in Eq. (4.4), as one approaches the long time limit, the strength of the interaction diverges logarithmically, regardless of how small the initial deviation is. For even higher scaling dimensions, $\alpha > 1$, the divergence becomes more severe. For any scaling, $\alpha \geq 1$, perturbation theory will eventually become inadequate at describing the long time dynamics and a non-perturbative treatment will then be required.

To illustrate this point further, we consider the result of time dependent perturbation theory on the dynamics of the effective moment of inertia, $\langle x^2 \rangle(\tau)$, when $\alpha = 1$. To second order in the interaction, the moment of inertia will have the form:

$$\begin{aligned}
\langle x^2 \rangle(\tau) &= A + B \frac{\lambda_0}{a} \log \left(\frac{1}{\pi/2 - \tau} \right) \sin(2\tau) \\
&+ D \frac{\lambda_0^2}{a^2} \log^2 \left(\frac{1}{\pi/2 - \tau} \right) + \dots \tag{4.5}
\end{aligned}$$

In Eq. (4.5) the coefficients A , B , and D depend on the zeroth, first, and second order expansions of Eq. (4.3), in terms of the interaction, respectively. The term proportional to $(\lambda_0/a)^0$ is the scale invariant result in Eq. (3.9). The term linear in λ_0/a is only important at short times because $\sin(2\tau)$ vanishes as λ_0^2/t , in the long time limit. Therefore at sufficiently long times the term linear in λ_0/a will disappear while the quadratic term diverges. For this reason, it is necessary to develop a non-perturbative treatment to the breaking of scale invariance.

As shown in Appendix B, it is possible to explicitly determine the leading long time behaviour of the time-ordering operator in Eq. (4.3), when $\alpha \geq 1$:

$$\begin{aligned} \lim_{\tau \rightarrow \pi/2} T e^{-i \int_0^\tau d\tau' \delta \tilde{H}_I(\tau')} &\approx \\ \exp\left(i \frac{\lambda_0}{a} \tilde{V}_I \log(\pi/2 - \tau)\right), &\quad \alpha = 1, \\ \exp\left(-i \tilde{V}_I \left(\frac{\lambda_0}{a}\right)^\alpha \frac{1}{\alpha - 1} \frac{1}{(\pi/2 - \tau)^{\alpha-1}}\right), &\quad \alpha > 1, \end{aligned} \quad (4.6)$$

where the operator, \tilde{V}_I , is the many body deviation from scale invariance in the interaction picture, evaluated at $\tau = \pi/2$:

$$\tilde{V}_I = e^{i\tilde{H}_s \pi/2} \delta \tilde{h} e^{-i\tilde{H}_s \pi/2}. \quad (4.7)$$

This matrix is universal, time-independent and dimensionless. The concrete form of \tilde{V}_I only depends on the number of particles involved, N . Eq. (4.6) leads to the following expression for the expansion coefficients:

$$\begin{aligned} C_n(\tau) &\approx \\ \langle n | \exp\left(i \frac{\lambda_0}{a} \tilde{V}_I \log(\pi/2 - \tau)\right) | \psi_0 \rangle, &\quad \alpha = 1, \\ \langle n | \exp\left(-i \tilde{V}_I \left(\frac{\lambda_0}{a}\right)^\alpha \frac{1}{\alpha - 1} \frac{1}{(\pi/2 - \tau)^{\alpha-1}}\right) | \psi_0 \rangle, &\quad \alpha > 1. \end{aligned} \quad (4.8)$$

The solution to the unitary dynamics in the non-inertial reference frame, Eqs. (4.6), (4.7), and (4.8), is equivalent to a time-independent problem with Hamiltonian, \tilde{V}_I , and time coordinate, $-\log(\pi/2 - \tau)$ for $\alpha = 1$, and $(\pi/2 - \tau)^{\alpha-1}$ for $\alpha > 1$. In the non-inertial reference frame, the long time dynamics will exhibit oscillations which can be determined by evaluating the spectrum of \tilde{V}_I . These deviations will explicitly break the simple scaling dynamics observed at scale invariant fixed points, Eqs. (3.7).

In addition, it follows from Eq. (4.6) and Eq. (4.8) that any local operator, $O(\{\vec{r}_i\})$, with scaling dimension, d_O , will have the following dynamics in the laboratory frame:

$$\begin{aligned} \lim_{t \rightarrow \infty} \langle O \rangle(t) &\approx \frac{1}{\lambda(t)^{d_O}} F\left(\left(\frac{\lambda_0}{a}\right) \log(t/\lambda_0^2)\right), &\quad \alpha = 1, \\ &\approx \frac{1}{\lambda(t)^{d_O}} F\left(\left(\frac{\lambda_0}{a}\right)^\alpha \frac{1}{\alpha - 1} (t/\lambda_0^2)^{\alpha-1}\right), &\quad \alpha > 1, \end{aligned} \quad (4.9)$$

where $F(t)$ is a dimensionless function. Although the specific form of $F(t)$ depends on the observable and the spectrum of the matrix, \tilde{V}_I , here we stress that the argument of this function is set only by the scaling of the deviation operator, α . In comparison to the result for scale

invariant systems, Eq. (3.8), the long time dynamics are no longer related to a simple time dependent rescaling, but now have a non-trivial time dependence.

A similar analysis is valid when $\alpha < 1$. In this case, the deviations from scale invariance will vanish in the long time limit. The dynamics in the non-inertial frame will quickly freeze, and the dynamics in the laboratory frame will become a simple time dependent rescaling, Eq. (3.7). The only difference is that the profile of the wave function will be altered by the presence of interactions. The effect of the interactions on the expansion coefficients is well described by time dependent perturbation theory:

$$C_n(\tau) \approx C_n(0) - i \left(\frac{\lambda_0}{a}\right)^\alpha \int_0^\tau d\tau' \sec^\alpha(\tau') \langle n | e^{i\tilde{H}_s \tau'} \delta \tilde{h} e^{i\tilde{H}_s \tau'} | \psi_0 \rangle. \quad (4.10)$$

Eqs. (4.6), (4.7), (4.8), (4.9), and (4.10) are the main theoretical results of this paper. These results are valid for any non-relativistic, Galilean invariant quantum system close to a scale invariant fixed point. These results do not depend on the number of particles, or their statistics, only on the scaling of the deviation, α .

The remainder of this work will be focused on applying this formalism to study the dynamics of two systems, the non-interacting quantum gas in the presence of an impurity, and the two-body problem. In these cases, the deviation we consider occurs because the potentials are nearly scale invariant. For such systems, the deviation can be written in the form:

$$\begin{aligned} \delta \tilde{H}(\tau) &= \frac{1}{2} \sum_{i,j} \lambda^2(\tau) V(\lambda(\tau)(\vec{x}_i - \vec{x}_j)) - V_s(\vec{x}_i - \vec{x}_j) \\ &+ \sum_i \lambda^2(\tau) U(\lambda(\tau)\vec{x}_i) - U_s(\vec{x}_i). \end{aligned} \quad (4.11)$$

V. DYNAMICS OF A NON-INTERACTING QUANTUM GAS IN THE PRESENCE OF AN IMPURITY

We now apply the formalism of Sec. IV to the dynamics of a non-interacting quantum gas in the presence of a short ranged, immobile impurity, in three spatial dimensions. The effect of the impurity is to create an external potential for the quantum gas. The effective Hamiltonian for the system, is given by Eq. (2.9), with the interparticle interaction, $V(\vec{x})$, set to zero. Since the quantum gas is non-interacting, it is only necessary to consider the motion of a single particle. The extension to multiple particles is discussed at the end of this section.

In this analysis we consider a spherically symmetric, impurity potential with a finite range, $r_0 \ll \lambda_0$. Since angular momentum is a good quantum number for these potentials, the scattering in different angular momentum channels will be decoupled. At low energies, only the zero angular momentum scattering will be appreciable.

The s-wave scattering will introduce a new length scale into the system, the scattering length, a . When a is finite the scale invariance is broken, but the symmetry is restored when the system is non-interacting, $a = 0$, or at resonance, $a = \infty$.

To facilitate our study, we also consider a wave function which is a superposition of only s-wave states with initially real expansion coefficients. This assumption is made to clearly highlight the departure from scale invariance on the dynamics near the resonant and non-interacting fixed points.

A. Near Resonance

For large scattering lengths, we expand the total Hamiltonian around the resonant Hamiltonian. The eigenstates of the resonant Hamiltonian can be evaluated analytically, and are given by:

$$\phi_n(\vec{x}) = \langle x|n\rangle = \sqrt{\frac{1}{2\pi}} \frac{1}{x} \phi_{h.o.,2n}(x), \quad E_n = 2n + 1/2, \quad (5.1)$$

where $\phi_{h.o.,n}(x)$ is a one dimensional harmonic oscillator eigenstate with quantum number, $n = 0, 1, 2, \dots$ and a harmonic length of unity. The resonant eigenstates form a conformal tower, as is required by the scale invariance of the Hamiltonian in the laboratory frame.

In order to determine the matrix elements of the deviation, Eq. (4.11), it is necessary to examine the short distance behaviour of the wave function [45, 46]. The explicit calculation is shown in Appendix A, here we simply state the result:

$$\langle m|\delta\tilde{H}(\tau)|n\rangle = -\frac{\lambda_0}{4\pi a} \sec(\tau) \phi_{h.o.,2m}(0) \phi_{h.o.,2n}(0). \quad (5.2)$$

This result is consistent with the scaling, $\alpha = 1$.

Applying the results of Sec. IV for $\alpha = 1$, the expansion coefficients can be written as:

$$C_n(\tau) \approx \langle n|\exp\left(i\frac{\lambda_0}{4\pi a}\tilde{V}_I \log(\pi/2 - \tau)\right)|\psi_0\rangle, \quad (5.3)$$

where \tilde{V}_I is given by Eqs. (4.7) and (5.2). The resonant matrix elements of \tilde{V}_I are:

$$\langle n|\tilde{V}_I|m\rangle = f_n f_m \quad f_n = \frac{\sqrt{2}}{\pi^{1/4}} \frac{(2n-1)!!}{\sqrt{(2n)!}}. \quad (5.4)$$

The spectrum of \tilde{V}_I can be determined by noting that each matrix element of \tilde{V}_I is a product of two factors. For these separable matrices, there is a single non-zero eigenvalue, v , with eigenstate, $|v\rangle$:

$$v = Tr\tilde{V}_I = \sum_n f_n^2 \quad \langle n|v\rangle = \frac{f_n}{\sqrt{v}}. \quad (5.5)$$

The eigenvalue, v , diverges with the harmonic quantum number as: \sqrt{n} . We note that this sum is controlled by the energy scale set by the range of the potential: $n_{max} = r_0^{-2}\lambda_0^2$, where r_0 is the range of the potential with $r_0 \ll a$.

Inserting a complete set of eigenstates for \tilde{V}_I allows one to simplify Eq. (5.3):

$$\begin{aligned} \lim_{\tau \rightarrow \pi/2} C_n(\tau) &\approx \langle n|\psi_0\rangle \\ &+ 2i \exp\left(i\frac{v}{2}\frac{\lambda_0}{4\pi a} \log(\pi/2 - \tau)\right) \\ &\cdot \sin\left(\frac{v}{2}\frac{\lambda_0}{4\pi a} \log(\pi/2 - \tau)\right) \langle n|v\rangle \langle v|\psi_0\rangle \end{aligned} \quad (5.6)$$

The first term in Eq. (5.6) is the initial expansion coefficients, $C_n(0)$. When this term is substituted back into Eq. (4.3), it will produce the scale invariant dynamics. The presence of the second term will produce a beat in the probability density of the form $\sin^2(v\lambda_0/(4\pi a)\log(\pi/2 - \tau)/2)$, in the non-inertial reference frame, or $\sin^2(v\lambda_0/(4\pi a)\log(t/\lambda_0^2)/2)$, in the laboratory frame. The beat is illustrated in Fig. (1), where we show the numerical solution for the probability to be in the resonant ground state, $|C_0|^2$, for a wave function initially in the resonant ground state. The solution is obtained by numerically solving the time dependent Schrodinger equation, Eq. (2.9). The oscillations at frequency, $v/2$, are easily observed and are well described by Eq. (5.6).

The departure from scale invariance will affect all the quantum dynamics of the system. It is most easily observed when the overlap between the initial state and the state $|v\rangle$ is appreciable. For the overlap to be appreciable, it is necessary to consider a small, but finite, r_0 . In the zero-range limit, the projection of the eigenstate, $|v\rangle$, onto any conformal tower state vanishes like $v^{-1/2} \approx r_0$, see Eq. (5.5). Although the frequency of the log-periodic diverges in this limit, the amplitude of the beat vanishes like r_0^2 . As a result, in the truly zero-range limit the scale invariant dynamics are robust against deviations. For small, but finite r_0 , the departure from scale invariant dynamics will be most visible.

As an example of the effect of the log-periodic beat, the time evolution of the moment of inertia in the expanding non-inertial reference frame, $\langle x^2 \rangle$, is shown in Fig. (2). In terms of the laboratory frame, the dynamics of the moment of inertia are given by:

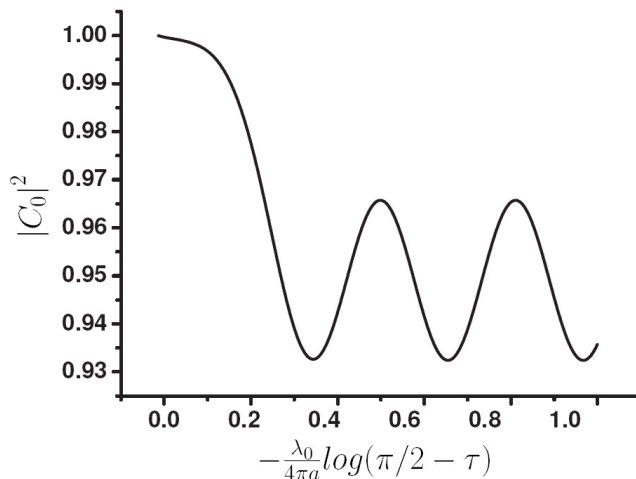


Figure 1: The probability for the particle to remain in the resonant ground state in the effective frame, for large finite scattering lengths, $a \gg \lambda_0$, as a function of $-\lambda_0/(4\pi a) \log(\pi/2 - \tau)$. This result has been obtained by numerically solving Eq. (4.3) with $\lambda_0/(4\pi a) = 0.015$ and $r_0/\lambda_0 = 10^{-3/2}$. The system is initially prepared in the ground state of the resonant model. Very quickly the probability satisfies Eq. (5.6), and develops oscillations at the frequency $v/2 = 20.14$.

$$\begin{aligned} \langle r^2 \rangle(t) &= \lambda^2(t) \langle x^2 \rangle(\tau(t)), \\ \lim_{t \rightarrow \infty} \langle x^2 \rangle(t) &\approx A + B \sin\left(v \frac{\lambda_0}{4\pi a} \log(t/\lambda_0^2)\right) \frac{\lambda_0^2}{t} \\ &\quad + D \sin^2\left(\frac{v}{2} \frac{\lambda_0}{4\pi a} \log(t/\lambda_0^2)\right). \end{aligned} \quad (5.7)$$

In Eq. (5.7), the coefficients A , B , and D depend on the initial conditions, and the range of the potential, r_0 , through the state $|v\rangle$. Explicit expressions for these coefficients are given in Appendix C. This result is consistent with Eq. (4.9) and is identical to the standard perturbation theory, Eq. (4.5), if one expands the sine functions to first order in $v\lambda_0/(4\pi a) \log(t/\lambda_0^2)$. The presence of the beat in the expansion coefficients can lead to significant deviations from the scale invariant dynamics, which can be seen in Fig. (2).

Eqs. (5.6), and (5.7) consider the motion of a single particle. The extension to multiple particles can be easily considered by examining all the possible ways for the N cold atoms to occupy the eigenstates of \tilde{V}_I . For fermions, the Pauli-exclusion principle prevents multiple fermions with the same spin to occupy the state, $|v\rangle$. This results in the appearance of a single frequency v in the dynamics. On the other hand, multiple bosons can occupy the state, $|v\rangle$, and thus the dynamics will have oscillations at the frequency, v , and its harmonics.

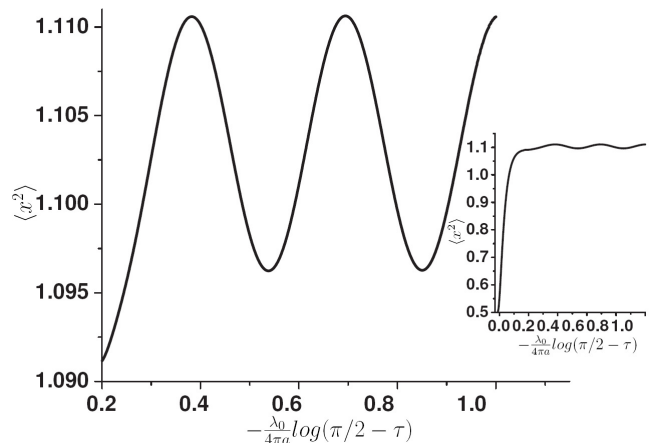


Figure 2: The time evolution of $\langle x^2 \rangle(\tau)$ as a function of $-\lambda_0/(4\pi a) \log(\pi/2 - \tau)$. This has been obtained by numerically solving the near resonant wave function, Eq. (4.3). In this calculation, the system was prepared in the ground state with $\lambda_0/(4\pi a) = 0.015$ and $r_0/\lambda_0 = 10^{-3/2}$. The dynamics can be fit to Eq. (5.7), with oscillations at frequency $v/2 = 20.14$. In the inset, the dynamics over the entire range is shown.

B. Weak Impurity Dynamics

For weak interactions, it is necessary to expand $\tilde{H}(\tau)$ around the non-interacting Hamiltonian, the eigenstates of which are:

$$\phi_n(\vec{x}) = \langle x|n\rangle = \sqrt{\frac{1}{2\pi} \frac{1}{x}} \phi_{h.o., 2n+1}(x), \quad E_n = 2n + 3/2. \quad (5.8)$$

The deviation from the non-interacting Hamiltonian can be found using the same methods as the resonant case, and is discussed in Appendix A:

$$\langle m|\delta\tilde{H}(\tau)|n\rangle = \frac{4\pi a}{\lambda_0} \cos(\tau) \phi'_{h.o., 2n+1}(0) \phi'_{h.o., 2m+1}(0), \quad (5.9)$$

which is consistent with $\alpha = -1$. As discussed in Sec. IV, the effects of the interaction vanish in the large time limit, $t \gg \lambda_0^2$, and there will be a well defined limit as τ approaches $\pi/2$. The resulting dynamics in the laboratory frame will then become a simple time dependent rescaling, Eq. (3.7). For such systems, the expansion coefficients at all times can be well described by first order perturbation theory, Eq. (4.10), for small deviations $a \ll \lambda_0$.

C. Trapped Impurity

So far the impurity has been assumed to be immobile. Practically, an impurity atom can never be truly immo-

bile thanks to zero point motion. Here we consider a more realistic set up: a quantum gas interacting with an impurity of mass, M , that is subjected to a harmonic trap of frequency..

In the laboratory frame, the Hamiltonian for the system is:

$$H = \sum_i -\frac{1}{2}\nabla_i^2 - \frac{1}{2M}\nabla_I^2 + \frac{1}{2}M\omega_I R_I^2 + \sum_i U(\vec{r}_i - \vec{R}_I), \quad (5.10)$$

where $U(\vec{r})$ is the short range atom-impurity interaction. In this Hamiltonian, the motion of the trapped impurity atom is included alongside the quantum gas. The operators, R_I and $-i\nabla_I$ are the coordinate and momenta operators for the impurity atom, while \vec{r}_i and $-i\nabla_i$ are still the coordinates and momenta for the quantum gas.

One can still use Eq. (2.2) to move to the expanding non-inertial reference frame. In order to examine the dynamics of the quantum gas, it is ideal to choose Eq. (2.8) as the solution for $\lambda(t)$. This choice of $\lambda(t)$ then gives the modified effective Hamiltonian:

$$\begin{aligned} \tilde{H} = \sum_i \left(-\frac{1}{2}\tilde{\nabla}_i^2 + \frac{1}{2}x_i^2 + \lambda^2(\tau)U(\lambda(\tau)(\vec{x}_i - \vec{X}_I)) \right) \\ - \frac{1}{2M}\tilde{\nabla}_I^2 + \frac{1}{2}MX_I^2 (\omega_I^2\lambda^4(\tau) + 1) \end{aligned} \quad (5.11)$$

where $\vec{X}_I = \vec{R}_I/\lambda(t)$.

Eq. (5.11) states that the impurity is subject to a harmonic trap of frequency: $\sqrt{\omega_I^2\lambda^4(\tau) + 1}$. As τ approaches $\pi/2$, the frequency of the trap will diverge. In this case, we expect that the motion of the impurity to be adiabatic, and that the impurity will become more and more localized near the origin.

To test this hypothesis, we show in Fig. (3) a) the probability for the impurity to be in the instantaneous ground state of the trap, when it was initially prepared in the ground state. It is easy to see that the adiabatic approximation works extremely well in the long time limit. The fluctuations in the position of the trapped impurity, $\sqrt{\langle X_I^2 \rangle}$, are then be related to the instantaneous trap size:

$$\sqrt{\langle X_I^2 \rangle} = \sqrt{\frac{1}{M\omega_I\lambda_0^2} \cos(\tau)}, \quad (5.12)$$

which vanishes in the long time limit. The dynamics of this expectation value is shown in Fig. (3) b).

The adiabatic dynamics in the non-inertial reference frame is intuitive when one considers the motion in the laboratory frame. For heavy impurities, or large trapping potentials, the interaction between the impurity and the gas will not excite the impurity. As a result, when the gas expands further away from the impurity, the impurity will remain near the origin, and it's exact position in

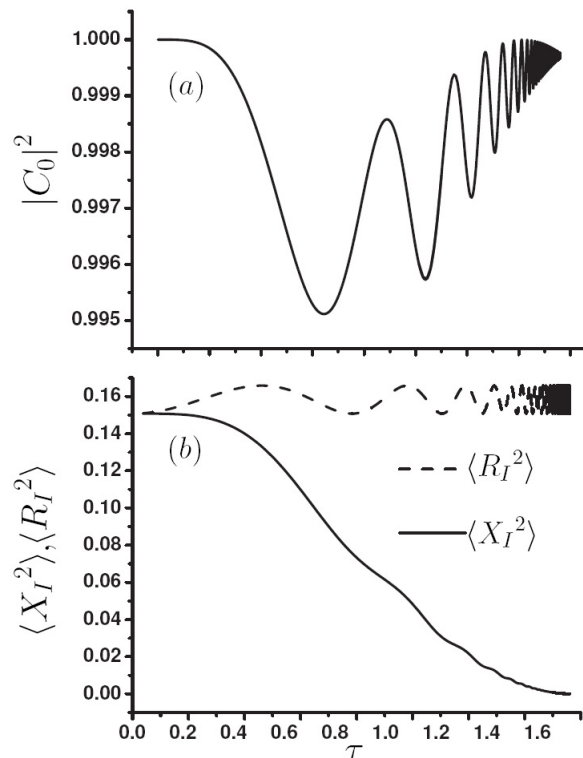


Figure 3: The time evolution of the trapped impurity according to Eq. (5.11) in units of λ_0 , for $M\omega_I\lambda_0^2 = 3$. a) The probability of being in the instantaneous ground state of Eq. (5.11). b) The fluctuations of the trapped impurity position, Eq. (5.12), in both the laboratory (dashed line) and non-inertial reference frames (solid line).

the trap will become more and more irrelevant to the expanding gas.

The adiabaticity of the impurity results in a form of coarse grained dynamics for the quantum gas. In the long time limit, the dynamics of the quantum gas will be insensitive to the initial preparation of the impurity. That is, all the results obtained for the immobile impurity will be equally valid for the trapped impurity when: $t \gg \lambda_0^2$.

VI. DYNAMICS OF A TWO-BODY SYSTEM

In this section we study the dynamics of two particles with short ranged s-wave interactions. The two particles can either be two bosons, two fermions in the spin singlet channel, or two distinguishable particles. The Hamiltonian in the non-inertial reference frame is given by Eq. (2.9), with the external potential, $U(\vec{x}_i)$, set to zero. We still focus on s-wave scattering, which is valid for low energies, and is parametrized by the scattering length, a . Again, scale invariance occurs at resonance, $a = \infty$, and when $a = 0$.

For two particles in the non-inertial reference frame one can separate the center of mass and relative motions. The Schrodinger equation for the relative motion is:

$$i \frac{\partial}{\partial \tau} \phi(\vec{x}, \tau) = \left(-\frac{1}{2\mu} \tilde{\nabla}^2 + \frac{1}{2} \mu x^2 + V(\lambda(\tau) \vec{x}) \right) \phi(\vec{x}, \tau), \quad (6.1)$$

where \vec{x} is the relative coordinate between the two particles in the non-inertial reference frame, and μ is the reduced mass.

Eq. (6.1) is nothing more than the Schrodinger equation for a single particle in an external potential, which was discussed in Sec. V. Therefore, all the dynamics for the relative motion will be equivalent to the motion of a single particle of reduced mass, μ , in the presence of an external potential. Near resonance, the leading behaviour of the expansion coefficients, Eq. (4.3), will be given by Eq. (5.6). The relative dynamics will then exhibit a log-periodic beat with a single finite range dependent frequency, Eq. (5.5). For example, the dynamics of the relative moment of inertia, $\langle r^2 \rangle(t)$, is simply Eq. (5.7). For weak interactions the dynamics in the laboratory frame will eventually become a simple rescaling, see Eq. (3.7).

In addition to these results, we note that the two-body interaction does not break translational invariance in the laboratory frame. Thus, it is meaningful to study the dynamics of the momentum distribution, $n(k, t)$. In particular, we examine the dynamics of the contact [45]. The contact is defined by the asymptotic behaviour of the momentum distribution: $C(t) = \lim_{k \rightarrow \infty} k^4 n(k, t)$. The dynamics of the contact at resonance, and for weak interactions has been discussed previously in Ref. [40]. Here we extend their analysis to study the dynamics of the contact near resonance.

In order to obtain the momentum distribution near resonance, we will assume an initial wave function that is a product state between the center of mass, and relative motion. One can then integrate out the center of mass coordinate trivially, and examine the momentum distribution for the relative coordinate. The relative momentum distribution for this case is related to the Fourier transform of the solution for the relative wave function, Eq. (4.3), in the laboratory frame:

$$\psi(k, t) = \sum_n \frac{1}{\lambda^{3/2}(t)} C_n(\tau) e^{-2in\tau} \int d^3 r e^{i \frac{r^2}{2} \frac{\lambda(t)}{\lambda(\tau)} - i \vec{k} \cdot \vec{r}} \phi_n \left(\frac{\vec{r}}{\lambda(t)} \right), \quad (6.2)$$

For large momenta, the integrand of Eq. (6.2) will be dominated by the contribution at short distances, $r \ll k^{-1}$. Using the explicit resonant eigenstates, Eq. (5.1), one can evaluate the contribution to the Fourier transform from $r \ll k^{-1}$, and obtain a final expression for the contact:

$$\begin{aligned} C(t) &= \lim_{k \rightarrow \infty} k^4 n(k, t) = \lim_{k \rightarrow \infty} k^4 |\psi(k, t)|^2, \\ &= \frac{1}{\lambda(t)} \tilde{C}(\tau(t)), \\ \tilde{C}(\tau) &= \left| \sum_n C_n(\tau) e^{-2in\tau} \frac{\sqrt{\pi}}{2} f_n \right|^2, \end{aligned} \quad (6.3)$$

where $C_n(\tau)$ is the expansion coefficients, defined in Eq. (5.6), and f_n in Eq. (5.4).

At resonance, the contact in the non-inertial reference frame, $\tilde{C}(\tau)$, tends to a constant which depends on the initial conditions. This result was obtained in Ref. [40]. Near resonance, however, the expansion coefficients are time dependent due to the log-periodic beat, Eq. (5.6). The beat in the expansion coefficients will translate to a beat in the contact:

$$\lim_{t \rightarrow \infty} C(t) \approx \frac{E}{\lambda(t)} + \frac{F}{\lambda(t)} \sin^2 \left(\frac{v}{2} \frac{\lambda_0}{4\pi a} \log \left(\frac{t}{\lambda_0^2} \right) \right), \quad (6.4)$$

where E and F are two coefficients, which are given explicitly in Appendix C, and have neglected terms that vanish as $(\lambda_0^2/t)^2$. The first term is the resonant scale invariant result, while the second term is the deviation that arises from breaking the scale invariance. Again, the presence of the log-periodic beat only depends on the deviation from resonance. The amplitude of the beat is controlled by the constant F which depends on the finite range, r_0 , through the state $|v\rangle$.

VII. DISCUSSION

The main result of this work is the formalism developed to describe the dynamics near different scale invariant fixed points, see Eqs. (4.2), (4.3), (4.6), (4.7), (4.8), and (4.9). In the context of cold gases, this approach is equally valid near both the non- and resonantly-interacting fixed points. The resulting dynamics near these fixed points can be qualitatively determined by the scaling of the deviation, Eq. (4.2). For deviations that have scaling dimension, $\alpha \geq 1$, the long time, $t \gg \lambda_0^2$, dynamics can not be described by perturbation theory. Instead, the long time behaviour of the wave function is encapsulated in a time-independent, universal matrix, \tilde{V}_I , given in Eq. (4.7). In the opposite limit, $\alpha < 1$, perturbation theory provides an accurate description of the dynamics. In this case, the wave function will freeze in the non-inertial reference frame, while the dynamics in the laboratory frame will become a simple rescaling, as seen in Eqs. (3.7) and (3.8).

This formalism was applied to the dynamics of both the non-interacting quantum gas in the presence of an impurity, and of the interacting two-body problem in

three spatial dimensions. Near resonance, a log-periodic beat appears in the expansion coefficients, Eq. (5.6), with a frequency which depends on the finite range of the interaction, Eq. (5.5). This beat will be manifest in the dynamics of the system, in the long time limit, see Eqs. (5.7), and (6.4). The amplitude of the beat will depend on the initial conditions and the range of the potential, r_0 .

The results summarized above fit nicely with the renormalization group idea of relevant and irrelevant perturbations [43, 44]. While relevant perturbations move the system away from a scale invariant fixed point in equilibrium physics, for dynamics we expect relevant deviations to break the scaling solutions in Eqs. (3.7), and (3.8). For three dimensional quantum gases, the perturbations near the non-interacting fixed point are irrelevant, while perturbations near the resonant fixed point are relevant. Our results show that the idea of relevancy is applicable to dynamics. Near the resonant fixed point, the relevant deviations give rise to the log-periodic beat, which breaks the scaling dynamics at the fixed point. This is in contrast to weak interactions, where the irrelevant deviations do not qualitatively affect the long time dynamics.

The notion of relevancy also allows one to compare the results discussed above with one dimensional systems with s-wave and p-wave interactions. For one dimensional s-wave systems, the non-interacting fixed point and resonant fixed point switch; i.e. the resonant fixed point is infra-red stable, while the weakly interacting fixed point is unstable. Repeating our calculation shows the dynamics agree with the relevancy of the perturbation. Namely, the scaling dimension of the deviation near the weakly interacting fixed point have scaling, $\alpha = 1$, and are thus relevant, while $\alpha = -1$, near the resonant fixed point. For p-wave interactions in one dimension, a renormalization group approach shows the physics should be identical to the three dimensional s-wave. We have repeated our calculation for p-wave interactions in one dimension. The dynamics for one dimensional p-wave interactions are identical to the three dimensional s-wave. All the results obtained for three dimensions will then apply to one dimensional systems.

The method employed in this work is general and can be applied to a wide variety of scale invariant and nearly scale invariant quantum systems. The cost for examining the dynamics in this expanding non-inertial reference frame is that the interactions become time dependent. The applicability of this method to many body systems lies in the ability to handle many body problems with time dependent interactions. Although this is a difficult task, the time dependence in the interference term of Eq. (4.8) depends only on the scaling of the interaction. This allows one to make scaling arguments for the expansion dynamics of strongly interacting quantum gases. The details of the dynamics will be encapsulated in the matrix, \tilde{V}_J , given in Eq. (4.7). We intend to examine the many body problem in a future work.

This work was funded by the National Science and

Engineering Research Council of Canada (Contract No. 288179), and the Canadian Institute for Advanced Research. The authors would like to thank Shao-Jian Jiang for helpful discussions.

Appendix A: Derivation of the Deviation Operator

In this appendix we derive the deviation, $\delta\tilde{H}(\tau)$, from the transformed scale invariant Hamiltonian, \tilde{H}_s , in the expanding non-inertial reference frame. The approach we employ here applies for both the non-interacting quantum gas with an impurity, and the relative dynamics of the two-body problem. The only difference is that in the two-body problem, one uses the reduced mass for the two particles. In both cases, the physical interaction will be some short ranged, spherically symmetric potential, $V(r)$.

We begin with the radial Schrodinger equation in the non-inertial reference frame:

$$\begin{aligned} i\partial_\tau\chi_l(x, \tau) &= \tilde{H}\chi_l(x, \tau), \\ \tilde{H} &= -\frac{1}{2}\partial_x^2 + \frac{1}{2}x^2 + \frac{l(l+1)}{2x^2} + \lambda^2(\tau)V(x\lambda(\tau)), \\ \lambda(\tau) &= \lambda_0 \sec(\tau), \end{aligned} \quad (\text{A.1})$$

where we have set the (reduced) mass to unity, and $Y_{l,m}(\vec{x})$ is the spherical harmonic with angular quantum number l and projection quantum number, m . The radial wave function, $\chi_l(x, \tau)$, is related to the full wave function via: $\psi_{l,m}(\vec{x}, \tau) = Y_{l,m}(\hat{x})\chi_l(x, \tau)/x$, and is properly normalized:

$$\int_0^\infty dx |\chi_l(x, \tau)|^2 = 1. \quad (\text{A.2})$$

In what follows we will only focus on the zero angular momentum, or s-wave, scattering of this potential, as higher angular momentum scattering is suppressed by a factor of $(\sqrt{E}r_0)^{2l}$, where r_0 is the range of the potential, and E is the energy.

For specificity, we will consider the potential to be a square well of depth: $V_0\lambda^2(\tau)$, and range: $r_0/\lambda(\tau)$. This potential is consistent with the time dependence of $\lambda^2(\tau)V(x\lambda(\tau))$, and captures all the essential physics at low energies. It is important to note that the range and depth of the potential are changing at a rate set by $\lambda(\tau)$, which is much slower than the energy scale set by the finite range of the potential, r_0 . This implies that we can use the adiabatic approximation. In this approximation, the effect of the finite scattering length is to impose the time dependent boundary condition at the range of the potential [45]:

$$\frac{\chi'(r_0/\lambda(\tau))}{\chi(r_0/\lambda(\tau))} = -\frac{\lambda(\tau)}{a}. \quad (\text{A.3})$$

As discussed in the main text, we split the effective Hamiltonian in the non-inertial reference frame, $\tilde{H}(\tau)$, into the effective Hamiltonian at the scale invariant fixed point, \tilde{H}_s , and a deviation, $\delta\tilde{H}(\tau)$:

$$\begin{aligned}\tilde{H}(\tau) &= \tilde{H}_s + \delta\tilde{H}(\tau), \\ \tilde{H}_s &= -\frac{1}{2}\partial_x^2 + \frac{1}{2}x^2 + \lambda^2(\tau)V_s(\lambda(\tau)x),\end{aligned}\quad (\text{A.4})$$

and $V_s(x)$ is a scale invariant potential. In this analysis the quantities of interest are the matrix elements of the deviation:

$$\begin{aligned}\delta\tilde{H}(\tau) &= \lambda^2(\tau)V(x\lambda(\tau)) - \lambda^2(\tau)V_s(\lambda(\tau)x), \\ \delta\tilde{H}(\tau) &= \lambda^2(\tau)V(x\lambda(\tau)) - V_s(x),\end{aligned}\quad (\text{A.5})$$

with respect to the eigenstates of \tilde{H}_s . In Eq. (A.5) we have used the fact that the system possesses scale invariance at a fixed point. This implies that $V_s(\lambda x) = \lambda^{-2}V_s(x)$. For more discussions on the role of scale invariance on the dynamics in the expanding non-inertial reference frame, see Sec. III.

We first evaluate the deviation from the resonant fixed point. The matrix elements of Eq. (A.5) near resonance can be determined by examining the zero angular momentum Schrodinger equation at, and near, resonance:

$$\begin{aligned}E_{r,n}\chi_{r,n}(x) &= \left(-\frac{1}{2}\partial_x^2 + \frac{1}{2}x^2 + V_{res}(x)\right)\chi_{r,n}(x), \\ E_m(\tau)\chi_m(x, \tau) &= \left(-\frac{1}{2}\partial_x^2 + \frac{1}{2}x^2 + \lambda^2(\tau)V(x/\lambda(\tau))\right)\chi_m(x, \tau). \quad \chi_{r,n}(\vec{x}) = \langle x|n\rangle = \sqrt{2}\phi_{h.o.,2n}(x), \quad E_{r,n} = 2n + 1/2,\end{aligned}\quad (\text{A.6})$$

The top and bottom lines correspond to the resonant and off resonant Schrodinger equations, respectively. The states $\chi_{r,n}(x)$ and $\chi_m(x, \tau)$ are the eigenstates of the system with energy $E_{r,n}$ and $E_m(\tau)$, and quantum numbers n and m , for the resonant, and off resonant Hamiltonians, respectively.

At this stage one can multiply the resonant (off-resonant) Schrodinger equation by the state $\chi_m(x, \tau)$ ($\chi_{r,n}(x)$), and integrate over the range of the potential, $r_0/\lambda(\tau)$. The difference between the two Schrodinger equations is:

$$\begin{aligned}&\int_0^{r_0/\lambda(\tau)} dx \chi_{r,n}(x)(E_m(\tau) - E_{r,n})\chi_m(x, \tau) = \\ &\int_0^{r_0/\lambda(\tau)} dx \chi_{r,n}(x) \left[-\frac{1}{2}\partial_x^2 + \frac{1}{2}x^2 + \lambda^2(\tau)V(x/\lambda(\tau))\right] \chi_m(x, \tau) \\ &- \int_0^{r_0/\lambda(\tau)} dx \chi_m(x, \tau) \left[-\frac{1}{2}\partial_x^2 + \frac{1}{2}x^2 + V_{res}(x)\right] \chi_{r,n}(x)\end{aligned}\quad (\text{A.7})$$

To obtain the deviation operator, we expand the difference to first order in $1/a$. To this order the expansion of Eq. (A.7) gives:

$$\begin{aligned}&\int_0^{r_0/\lambda(\tau)} dx (\lambda^2(\tau)V(x\lambda(\tau)) - V_{res}(x))\chi_{r,m}(x)\chi_{r,n}(x) = \\ &\int_0^{r_0/\lambda(\tau)} dx \{(E_m(\tau) - E_{r,n})\chi_m(x, \tau)\chi_{r,n}(x)\} \\ &- \frac{\lambda(\tau)}{2a}\chi_{r,m}(r_0/\lambda(\tau))\chi_{r,n}(r_0/\lambda(\tau)).\end{aligned}\quad (\text{A.8})$$

In Eq. (A.8) we have used Eq. (A.3) to evaluate the difference in kinetic energies.

In the second line of Eq. (A.8), the quantities $E_m(\tau) - E_{r,n}$ and $\chi_{r,n}(x)\chi_m(x, \tau)$ are to be expanded to first order in $\lambda(\tau)/a$. The integrals themselves will be proportional to $r_0/\lambda(\tau)$, for $r_0 \ll \lambda_0$. Therefore the second line in Eq. (A.8) will be a correction of order r_0/a to the matrix elements, and is thus negligible in the large scattering length limit. After neglecting the integrals, the expression for the deviation becomes:

$$\begin{aligned}\langle m|\delta\tilde{H}(\tau)|n\rangle &= \\ &\int_0^{r_0/\lambda(\tau)} (\lambda^2(\tau)V(x\lambda(\tau)) - V_{res}(x))\chi_{r,m}(x)\chi_{r,n}(x) \\ &= -\frac{\lambda(\tau)}{2a}\chi_{r,m}(r_0/\lambda(\tau))\chi_{r,n}(r_0/\lambda(\tau)).\end{aligned}\quad (\text{A.9})$$

To simplify the deviation further, we note that the resonant eigenstates outside the potential are given by:

where $\phi_{h.o.,n}(x)$ is the normalized one-dimensional harmonic oscillator wave function with quantum number $n = 0, 1, 2, \dots$, and with the harmonic length scale set to unity. For $x \ll 1$, the resonant eigenstates are nearly constant near the origin. The continuity of the wave function at the boundary allows one to simplify the deviation to:

$$\langle m|\delta\tilde{H}(\tau)|n\rangle = -\frac{\lambda(\tau)}{2a}\chi_{r,m}(0)\chi_{r,n}(0).\quad (\text{A.11})$$

This result is equivalent to Eq. (5.2) up to a factor of 4π .

In this case of weak interactions, we compare the non- and weakly-interacting Schrodinger equations in the non-inertial reference frame:

$$\begin{aligned}E_{0,n}\chi_{0,n}(x) &= \left(-\frac{1}{2}\partial_x^2 + \frac{1}{2}x^2\right)\chi_{0,n}(x), \\ E_m(\tau)\chi_m(x, \tau) &= \left(-\frac{1}{2}\partial_x^2 + \frac{1}{2}x^2 + \lambda^2(\tau)V(x/\lambda(\tau))\right)\chi_m(x, \tau).\end{aligned}\quad (\text{A.12})$$

Here $\chi_{0,n}(x)$ is a non-interacting eigenstate with energy $E_{0,n}$ and quantum number $n = 0, 1, 2, \dots$:

$$\chi_{0,n}(\vec{x}) = \langle x|n\rangle = \sqrt{2}\phi_{h.o.,2n+1}(x), \quad E_{0,n} = 2n + 3/2. \quad (\text{A.13})$$

A calculation identical to the resonant case yields:

$$\langle m|\delta\tilde{H}(\tau)|n\rangle = \frac{\alpha}{2\lambda(\tau)}\chi'_{0,m}(0)\chi'_{0,n}(0), \quad (\text{A.14})$$

which is equivalent to Eq. (5.9) up to a factor of 4π .

The approach used here is similar to Ref. [46]. The matrix elements of Eq. (A.11) and (A.14) have an important connection to the thermodynamic contact first examined in Ref. [45]. If one were to consider just the ground state expectation value of the deviation, Eq. (A.5), one would simply obtain the contact. Eq. (A.5) is then a natural extension of the idea of contact to a matrix. The relationship between the breaking of scale invariance and the contact in equilibrium physics has been discussed in Ref. [33].

Appendix B: Solutions for the Expansion Coefficients near a Fixed Point

In this section we analyse the time dependent expansion coefficients near an arbitrary scale invariant fixed point. Near a fixed point, the effective wave function is given by:

$$\begin{aligned} \phi(\{\vec{x}_i\}, \tau) &= \sum_n C_n(\tau) e^{-iE_n\tau} \phi_n(\{\vec{x}_i\}), \\ C_n(\tau) &= \langle n|T e^{-i\int_0^\tau d\tau' \delta\tilde{H}_I(\tau')} |\psi_0\rangle, \\ \delta\tilde{H}_I(\tau) &= e^{i\tilde{H}_s\tau} \delta\tilde{H}(\tau) e^{-i\tilde{H}_s\tau}. \end{aligned} \quad (\text{B.1})$$

In Eq. (B.1), $|\psi_0\rangle$ is the initial state, $\phi_n(\{\vec{x}_i\}) = \langle\{x_i\}|n\rangle$ is the eigenstate of the scale invariant Hamiltonian in the non-inertial reference frame, \tilde{H}_s , with energy, $E_n = 2n$ and $n = 0, 1, 2, \dots$. The deviation from the scale invariant Hamiltonian is given by $\delta\tilde{H}(\tau)$.

To evaluate the expansion coefficients, $C_n(\tau)$, it is necessary to expand the exponential in the second line of Eq. (B.1). Here we will examine the m th order for the expansion coefficient:

$$\begin{aligned} C_n^{(m)}(\tau) &= \frac{(-i)^m}{m!} \int_0^\tau d\tau_1 \dots \int_0^\tau d\tau_m \\ &\langle n|T \delta\tilde{H}_I(\tau_1) \dots \delta\tilde{H}_I(\tau_m) |\psi_0\rangle. \end{aligned} \quad (\text{B.2})$$

We can remove the time ordering operator, T , by choosing a specific ordering of the time coordinates in Eq. (B.2). Each possible ordering of the coordinates will

generate an equal contribution, eliminating the $m!$ factor in Eq. (B.2):

$$\begin{aligned} C_n^{(m)}(\tau) &= -i^m \sum_{l_1, \dots, l_m} \int_0^\tau d\tau_1 \dots \int_0^{\tau_{m-1}} d\tau_m \\ &\langle n|\delta\tilde{H}(\tau_1)|l_1\rangle \dots \langle l_{m-1}|\delta\tilde{H}(\tau_m)|l_m\rangle \\ &e^{2i(n-l_1)} \dots e^{2i(l_{m-1}-l_m)} C_{l_m}(0), \end{aligned} \quad (\text{B.3})$$

where we have inserted $m - 1$ complete set of scale invariant eigenstates, and defined:

$$|\psi_0\rangle = \sum_l C_l(0)|l\rangle, \quad (\text{B.4})$$

with $C_l(0)$ being the initial expansion coefficients.

To make further progress, it is necessary to examine the time dependence of the deviation. For the cases under consideration, we write the deviation as:

$$\delta\tilde{H}(\tau) = \delta\tilde{h}\lambda^\alpha(\tau), \quad (\text{B.5})$$

where $\delta\tilde{h}$ is an operator that contains the matrix structure of the deviation, and α is a constant such that $\lambda^\alpha(\tau)$ gives the time dependence of the deviation. The parameter, $\lambda(\tau)$, is given by:

$$\lambda(\tau) = \lambda_0 \sec(\tau), \quad 0 \leq \tau < \pi/2. \quad (\text{B.6})$$

The explicit forms of $\delta\tilde{H}(\tau)$ near the resonant and non-interacting fixed points were derived in Appendix A. A quick inspection of the calculated deviations, Eqs. (A.11) and (A.14), shows that Eq. (B.5) is accurate.

The long time dynamics, $t \gg \lambda_0^2$, are determined by the behaviour of the deviation near $\tau = \pi/2$. This limit will depend on the scaling of the deviation, α . Motivated by the results of appendix A, we consider the cases when: $\alpha \geq 1$, and $\alpha < 1$.

1. $\alpha \geq 1$

For the case $\alpha \geq 1$, the deviation diverges as a function of time as:

$$\lambda^\alpha(\tau) \approx \frac{1}{(\pi/2 - \tau)^\alpha}. \quad (\text{B.7})$$

This implies that the dominant contribution to the expansion coefficients in the long time limit, $t \gg \lambda_0^2$, will be from $\tau \approx \pi/2$. In this limit, the time dependence from the exponential factors in Eq. (B.3) are irrelevant as they do not generate any divergences. For these terms, it is safe to set $\tau = \pi/2$. Most of the phase factors then reduce to unity, and one simply has to evaluate:

2. $\alpha < 1$

$$C_n^{(m)}(\tau) \approx -i^m \lambda_0^m \sum_{l_m} \langle n | \delta \tilde{h}^m | l_m \rangle e^{2i(n-l_m)} C_{l_m}(0) \\ \int_0^\tau d\tau_1 \dots \int_0^{\tau_{m-1}} d\tau_m \frac{1}{(\pi/2 - \tau_1)^\alpha} \dots \frac{1}{(\pi/2 - \tau_m)^\alpha}. \quad (\text{B.8})$$

Eq. (B.8) is equivalent to a long time expansion of the coefficients, C_n , and is valid up to corrections of λ_0^2/t . If one were to evaluate Eq. (B.8) for perturbations with scalings, $0 < \alpha < 1$, one would find that the dominant contribution to the integrals is from short times. In this case, the dynamics will be similar to the case when $\alpha < 0$, which will be discussed shortly.

The leading long time behaviour of the expansion coefficients, Eq. (B.8), for $\alpha \geq 1$, can be readily evaluated to give:

$$\int_0^\tau d\tau_1 \dots \int_0^{\tau_{m-1}} d\tau_m \frac{1}{(\pi/2 - \tau_1)^\alpha} \dots \frac{1}{(\pi/2 - \tau_m)^\alpha} \\ = \frac{1}{m!} \log^m \left(\frac{1}{\pi/2 - \tau} \right), \quad \alpha = 1 \\ = \frac{1}{m!} \left(\frac{1}{\alpha - 1} \frac{1}{(\pi/2 - \tau)^{\alpha-1}} \right)^m, \quad \alpha > 1 \quad (\text{B.9})$$

We now arrive at the final expression for the m th order of the expansion coefficient:

$$C_n^{(m)}(\tau) \\ \approx \frac{1}{m!} \langle n | \left(i \lambda_0 \tilde{V}_I \log(\pi/2 - \tau) \right)^m | \psi_0 \rangle, \quad \alpha = 1, \\ \approx \frac{1}{m!} \langle n | \left(-i \tilde{V}_I \frac{\lambda_0^\alpha}{\alpha - 1} \left(\frac{1}{\pi/2 - \tau} \right)^{\alpha-1} \right)^m | \psi_0 \rangle, \quad \alpha > 1, \quad (\text{B.10})$$

where we have defined:

$$\tilde{V}_I = e^{iH_s \pi/2} \delta \tilde{h} e^{-iH_s \pi/2}. \quad (\text{B.11})$$

With the aid of Eqs. (B.10) and (B.11), it is possible to obtain the full expansion coefficient, valid in the large time limit, $t \gg \lambda_0^2$:

$$C_n(\tau) = \sum_m C_n^{(m)}(\tau) \\ \approx \langle n | \exp \left(i \lambda_0 \tilde{V} \log(\pi/2 - \tau) \right) | \psi_0 \rangle, \quad \alpha = 1, \\ \approx \langle n | \exp \left(-i \tilde{V} \frac{\lambda_0^\alpha}{\alpha - 1} \frac{1}{(\pi/2 - \tau)^{\alpha-1}} \right) | \psi_0 \rangle, \quad \alpha > 1. \quad (\text{B.12})$$

When $\alpha < 1$, the deviation vanishes at large times, i.e. when τ tends to $\pi/2$. For sufficiently small deviations, i.e. for small scattering lengths $a \ll \lambda_0$, first order perturbation theory is sufficient at capturing the dynamics for all times:

$$C_n(\tau) = C_n(0) \\ - i \left(\frac{4\pi a}{\lambda_0} \right)^\alpha \int_0^\tau d\tau' \cos^\alpha(\tau') \langle n | e^{i\tilde{H}_s \tau'} \delta \tilde{h} e^{i\tilde{H}_s \tau'} | \psi_0 \rangle. \quad (\text{B.13})$$

The expansion coefficients for $\alpha < 1$ will have a well defined long time limit: $\lim_{\tau \rightarrow \pi/2} C_n(\tau) = C_n(\pi/2)$. For this reason, the wave function in the expanding non-inertial reference frame will eventually freeze. The only effect of the interactions will be to alter the profile of the wave function.

Appendix C: Beat Amplitudes for Moment of Inertia and Contact

In the previous appendix, the dynamics of the wave function were evaluated near resonance. In this appendix we report the analytic expressions for the long time, $t \gg \lambda_0^2$, or equivalently, $\tau \approx \pi/2$, dynamics the moment of inertia and for the contact, near resonance.

The long time asymptotics of the moment of inertia, in the non-inertial reference frame, is:

$$\lim_{t \rightarrow \infty} \langle x^2 \rangle(t) \approx A + B \sin \left(v \frac{\lambda_0}{a} \log(t/\lambda_0^2) \right) \frac{\lambda_0^2}{t} \\ + D \sin^2 \left(\frac{v}{2} \frac{\lambda_0}{4\pi a} \log(t/\lambda_0^2) \right). \quad (\text{C.1})$$

The coefficients A , B , and D are found by explicitly evaluating the expectation value. Here we quote the result:

$$A = \sum_{n=0}^{n_{max}} (2n + \frac{1}{2}) C_n^2(0) + \sum_{n=1}^{n_{max}} \sqrt{(2n)(2n-1)} C_n(0) C_{n-1}(0), \quad (C.2)$$

$$B = 2 \sum_{n=1}^{n_{max}} \sqrt{(2n+1)(2n+2)} (C_n(0) \langle n-1|v \rangle \langle v|\psi_0 \rangle - C_{n-1}(0) \langle n|v \rangle \langle v|\psi_0 \rangle), \quad (C.3)$$

$$D = \sum_{n=0}^{n_{max}} 2(2n + \frac{1}{2}) (C_n(0) \langle n|v \rangle \langle v|\psi_0 \rangle + |\langle n|v \rangle \langle v|\psi_0 \rangle|^2) - \sum_{n=1}^{n_{max}} 2\sqrt{(2n)(2n+1)} (C_n(0) \langle n-1|v \rangle \langle v|\psi_0 \rangle + C_{n-1}(0) \langle n|v \rangle \langle v|\psi_0 \rangle - 2\langle n|v \rangle \langle v|\psi_0 \rangle \langle n-1|v \rangle \langle v|\psi_0 \rangle). \quad (C.4)$$

In Eqs. (C.2), (C.3), and (C.4), $|\psi_0\rangle$, is the initial state, $C_n(0)$ is the initial expansion coefficients for $|\psi_0\rangle$, and $n_{max} = r_0^{-2} 2/\lambda_0^2$. The frequency, v , is the eigenvalue associated with the eigenstate $|v\rangle$, and are defined as:

$$v = \sum_n f_n^2 \quad \langle n|v \rangle = \frac{f_n}{\sqrt{v}}. \quad (C.5)$$

Similarly, we quote the results for the contact. The asymptotic form of the contact is:

$$\lim_{t \rightarrow \infty} C(t) \approx \frac{E}{\lambda(t)} + \frac{F}{\lambda(t)} \sin^2 \left(\frac{v}{2} \frac{\lambda_0}{4\pi a} \log \left(\frac{t}{\lambda_0^2} \right) \right). \quad (C.6)$$

The coefficients, E and F , are given by:

$$E = \left| \sum_{n=0}^{n_{max}} f_n \frac{\sqrt{\pi}}{2} (-1)^n C_n(0) \right|^2, \quad (C.7)$$

$$F = \left| \sum_{n=0}^{n_{max}} f_n \sqrt{\pi} (-1)^n \langle n|v \rangle \langle v|\psi_0 \rangle \right|^2 - \sum_{n,n'=0}^{n_{max}} \frac{\pi}{2} f_n f_{n'} (-1)^{n-n'} \cdot (C'_n(0) \langle n|v \rangle \langle v|\psi_0 \rangle + C_n(0) \langle n'|v \rangle \langle v|\psi_0 \rangle). \quad (C.8)$$

-
- [1] E. A. Donley, N. R. Claussen, S. L. Cornish, J. L. Roberts, E. A. Cornell and C. E. Wieman, *Nature* **412**, 295 (2001).
- [2] C. Chin, R. Grimm, P. Julienne, and E. Tiesinga, *Rev. Mod. Phys.* **82**, 1225 (2010).
- [3] A. Polkovnikov, K. Sengupta, A. Silva, M. Vengalattore, *Rev. Mod. Phys.* **83**, 863 (2011).
- [4] P. Makotyn, C. E. Klauss, D. L. Goldberger, E. A. Cornell, and D. S. Jin, *Nat. Phys.* **10**, 116 (2014).
- [5] M. Gring, M. Kuhnert, T. Langen, T. Kitagawa, B. Rauer, M. Schreitl, I. Mazets, D. Adu Smith, E. Demler, J. Schmiedmayer, *Science* **14**, 1318 (2012).
- [6] M. Schreiber, S. S. Hodgman, P. Bordia, H. P. Luschen, M. H. Fischer, R. Vosk, E. Altman, U. Schneider, and I. Bloch, *Science* **21**, 6250 (2015).
- [7] A. M. Kaufman, M. E. Tai, A. Lukin, M. Rispoli, R. Schittko, P. M. Preiss, M. Greiner, *Science* **19**, 794 (2016).
- [8] G. Jotzu, M. Messer, R. Desbuquois, M. Lebrat, T. Uehlinger, D. Greif and T. Esslinger, *Nature* **515**, 237 (2014).
- [9] F. Meinert, M. J. Mark, K. Lauber, A. J. Daley, and H.C. Nagerl, *Phys. Rev. Lett.* **116**, 205301 (2016).
- [10] A. Eckardt, *Rev. Mod. Phys.* **89**, 011004 (2017).
- [11] R. A. Barankov, L. S. Levitov, and B. Z. Spivak, *Phys. Rev. Lett.* **93**, 160401 (2004).
- [12] M. Heyl, A. Polkovnikov, and S. Kehrein, *Phys. Rev. Lett.* **110**, 135704 (2013).
- [13] M. S. Foster, V. Gurarie, M. Dzero, and E. A. Yuzbashyan, *Phys. Rev. Lett.* **113**, 076403 (2014).
- [14] A. Pal, D. A. Huse, *Phys. Rev. B* **82**, 174411 (2010).
- [15] T. Yefsah, R. Desbuquois, L. Chomaz, K. J. Gunter, and J. Dalibard, *Phys. Rev. Lett.* **107**, 130401 (2011).
- [16] C.-L. Hung, X. Zhang, N. Gemelke, and C. Chin, *Nature* **470**, 236 (2011).
- [17] E. Vogt, M. Feld, B. Frohlich, D. Pertot, M. Koschorreck, and M. Kohl, *Phys. Rev. Lett.* **108**, 070404 (2012).
- [18] K. Fenech, P. Dyke, T. Peppler, M G. Lingham, S. Hoinka, H. Hu, and C. J. Vale, *Phys. Rev. Lett.* **116**, 045302 (2016).
- [19] K. M. O'Hara, S. L. Hemmer, M. E. Gehm, S. R. Granade, and J. E. Thomas, *Science* **13**, 2179 (2002).
- [20] C. Cao, E. Elliott, J. Joseph, H. Wu, J. Petricka, T. Schafer, and J. E. Thomas, *Science*, **07**, 6013 (2011).
- [21] M. J. H. Ku, A. T. Sommer, L. W. Cheuk, and M. W. Zwierlein, *Science* **03**, 563 (2012).
- [22] S. J. Jiang, and F. Zhou, arXiv:1704.07557.
- [23] Y. Nishida, and D. T. Son, *Phys. Rev. Lett.* **97**, 050403 (2006).
- [24] S.J. Jiang, W.M. Liu, G. W. Semenoff, and F. Zhou, *Phys. Rev. A* **89**, 033614 (2014).
- [25] Y. Castin and R. Dum, *Phys. Rev. Lett.* **77**, 5315 (1996).
- [26] Y. Kagan, E. L. Surkov, and G. V. Shlyapnikov, *Phys. Rev. A* **54**, R1753 (1996).
- [27] F. Dalfovo, C. Minniti, S. Stringari, and L. Piatevskii, *Phys. Lett A* **227**, 259 (1997).

- [28] C. Menotti, P. Pedri and S. Stringari, Phys. Rev. Lett. **89**, 250402 (2002).
- [29] F. Dalfovo, S. Giorgini, L. P. Pitaevskii, and S. Stringari, Rev. Mod. Phys. **71**, 463.
- [30] J. Maki, S. J. Jiang, and F. Zhou, European Physics Letters, **118**,56002 (2017).
- [31] L.P. Pitaevskii and A. Rosch, Phys. Rev. A **55**, R853(R) (1997).
- [32] M. Olshanii, H. Perrin, and V. Lorent, Phys. Rev. Lett. **105**, 095302 (2010).
- [33] J. Hofmann Phys. Rev. Lett. **108**, 185303 (2012).
- [34] C. Gao, and Z. Yu, Phys. Rev. A **86**, 043609 (2012).
- [35] E. Taylor, and M. Randeria, Phys. Rev. Lett. **109**, 135301 (2012).
- [36] F. Chevy, V. Bretin, P. Rosenbusch, K. W. Madison, and J. Dalibard, Phys. Rev. Lett. **88**, 250402 (2002).
- [37] S. Deng, Z.Y. Shi, P. Diao, Q. Yu, H. Zhai, R. Qi, and H. Wu, Science **22**, 371 (2016).
- [38] S. E. Gharashi, and D. Blume, Phys. Rev. A **94**, 063639 (2016).
- [39] Y. Castin, Comptes Rendus Physique **5**, 407 (2004); F. Werner, Y. Castin, Phys. Rev. A **74**, 053604 (2006).
- [40] C. Qu, L. P. Pitaevskii, and S. Stringari, Phys. Rev. A **94**, 063635 (2016).
- [41] A. Minguzzi and D. M. Gangardt, Phys. Rev. Lett. **94**, 240404 (2005).
- [42] S. Moroz, Phys. Rev. A **86**, 011601(R) (2012).
- [43] K. G. Wilson, Ref. Mod. Phys. **55**, 583 (1983).
- [44] S. Sachdev, *Quantum Phase Transitions*, (Cambridge University Press 2011).
- [45] S. Tan, Ann. of Phys. **323**, 2952 (2008); Ann. of Phys. **323**, 2971 (2008).
- [46] S. Zhang, and A. Leggett, Phys. Rev. A **79**, 023601 (2009).
- [47] S.J. Jiang, J. Maki, and F. Zhou, Phys. Rev. A **93**, 043605 (2016).
- [48] V. Gritsev, P. Barmettler, and E. Demler, New Journal of Physics, **12**, 113005 (2010).
- [49] C. R. Hagen, Phys. Rev. D **5**, 377 (1972).
- [50] U. Niederer, helv. Phys. Acta **45**, 802 (1972).
- [51] Y. Nishida, and D. T. Son, Phys. Rev. D **76**, 086004 (2007).
- [52] From this point on we neglect the spin coordinate. The inclusion of spin in the following study is straightforward.
- [53] J. J. Sakurai, and J. Napolitano, *Modern Quantum Mechanics*, (Addison-Wesley 2011).